Politecnico di Milano

Scuola di Ingegneria Industriale e dell'Informazione

Corso di Laurea Magistrale in Automazione

Thesis
Title

Advisor: Prof. Name SURNAME
Co-Advisor: Dr. Name SURNAME
               Eng. Name SURNAME

Thesis by:
Name SURNAME   Matr. 000000

Academic Year 2016–2017

To someone very special. . .

Acknowledgments

Abstract

Nowadays...

Sommario

Contents

List of Figures

List of Tables

Introduction

Chapter 1

Introduction

"All models are wrong, but some are useful."

George Box

1.1   Motivation

Close range proximity operations between Spacecraft (S/C)s has been studied and discussed by space agencies and private companies since the early stages of space exploration, dating back to the Apollo program [?].

Since then we can find a wide range of missions where close-range proximity operations are in, like Formation Fliying (FF) [?] [?], On-Orbit Servicing (OOS) [?] [?] [?] [?] and Active Debris Removal (ADR) [?] [?].

Most of those missions were possible thanks to the presence of on-board crew or to the cooperativeness between S/Cs.

A target space object is deemed cooperative if it is built to provide information suitable for the estimation of its distance and orientation in space with respect to the chaser S/C. Also, it can be be actively or passively cooperative depending on whether it interacts with a dedicated radio-link with the chaser S/C or not [?].

As regard to the new generation of space robotics missions such as debris removal and OOS, proximity operations and docking are key-enabling capabilities for either repair, refuel or deorbit end-of-life and nonfunctional S/Cs [?].

The main challenge when performing close-range navigation in actual OOS and ADR removal missions however is when the target S/C may be uncooperative.

This implies that the target S/C may not be equipped with an active communication link or identifiable markers such as light-emitting diodes or corner cube reflectors to help with computing the relative position and attitude of the active S/C (chaser) with respect to a uncooperative target space object [?].

Another important aspect, which comes out when dealing with uncooperative

targets, is that debris or operating S/Cs to be serviced may have suffered physical damages as well as optical degradation of their surfaces due to the prolonged exposure to the space environment, thus appearing different than expected [?].

Thus, when operating in close-proximity the attitude and the motion of the target S/C must be estimated in autonomy by exploiting the sensors available on the servicer S/C.

With regards to the technological aspects, Electro-Optical (EO) sensors have been identified as the best option for relative navigation in the foredescribed scenario [?] [?].

Either active Light Detection and Ranging (LIDAR) systems or passive monocular and stereo cameras can be used. The selection of the navigation sensor must consider the resources available on board in terms of mass, electrical and processing power, on one side, the mission scenario and the costs to be sustained for design and development of the satellite system, on the other side [?] [?].

As stated in [?] monocular vision navigation has been identified as an enabling technology for present and future FF and OOS missions (namely PROBA-3 by ESA [?], PRISMA by OHB Sweden [?]).

Monocular navigation on such missions relies on finding an estimate of the initial pose of the space resident object with respect to the camera, based on a minimum number of features from a 3D computer model and a single 2D image [?].

In contrast to other state-of-the-art systems based on Light Detection and Ranging (LIDaR) or stero camera sensors, monocular navigation ensures rapid pose determination while offering some advantages such as lower hardware complexity, cost, weight and power consumption, possibility to be simultaneously used for supervised applications and a much larger operational range, not limited by the size of the platform [?] [?] [?]. However, the benefit of lower hardware complexity trades off with increased algorithmic complexity since a monocular sensor cannot provide direct direct three-dimensional (3D) measurements about the target.

Moreover, monocular sensors can be less robust to adverse illumination conditions typical of the space environment [?] (e.g., saturation under direct Sun illumination, or absence of light during eclipse) [?].

The increasing challenges of space exploration and moreover the urgent need for debris removal to free slots in orbit and to avoid unwanted collisions is what mainly motivate this work.

The capability of being able to develop and test pose determination algorithm in fact will be a key factor for the overall success of new generation missions.

Thus, this work is motivated from the need to give to the space community a reliable and extendable Free, Libre and Open Source Software (FLOSS) solution for simulating spaceborne imagery for Computer-Vision (CV) alghoritms needs.

1.2   Problem Statement

As will be better explained in the following chapters, in order to verify the goodness of a given image dataset, the most meaningful way it is to apply on it a CV algorithm on it.

In this work so, we will validate the generated dataset by implementing the Sharma-Ventura-D'Amico (SVD) monocular pose initialization algorithm.

As stated in [?] and [?], the pose initialization problem consist of determining the position of the Center of Mass (CG) t_C and the orientation of the principal axes A_{BC} of a non-cooperative target S/C (no markers or other specific supportive means) with respect to the camera frame **C** from a single Two-Dimensional (2-D) image, given its Three-Dimensional (3-D) geometrical representation (referred as map or model).

If we assume that the 3-D model of the target S/C is defined in a body fixed coordinate system **T**, and it is aligned with the target's principal axes with its origin at the CG, the orientation is then defined by the Direction Cosine Matrix (DCM) A_{BC}, which represents the trasformation from the coordinate system of **T** to **C**
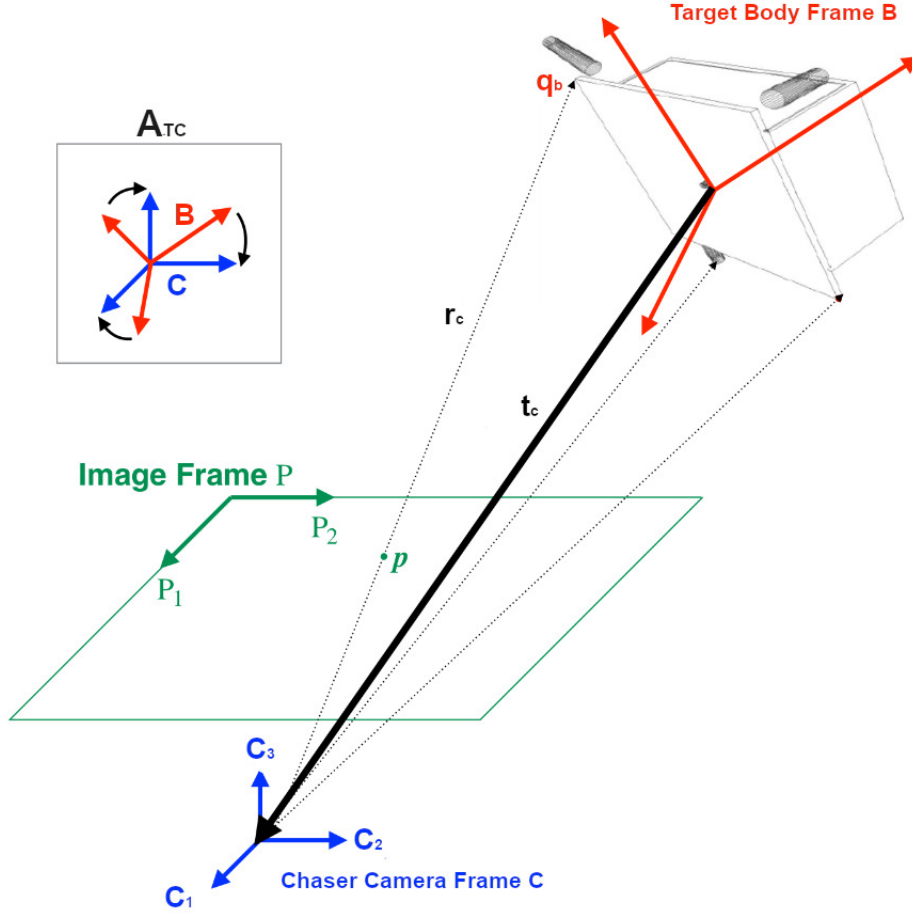
Figure 1.1: Schematic representation of the pose estimation problem using a monocular image [**?**]

A generic image point $p = [u, v]^T$ can be related to the corresponding $\mathbf{q_B}$ point of the 3-D model by means of the unknown pose ($t_C \ A_{BC}$) according to the following 2-D - 3-D true perspective equations:

$$\mathbf{r_C} = \begin{bmatrix} x_C & y_C & z_C \end{bmatrix}^T = \mathbf{A_{TC}} \ \mathbf{q_B} + \mathbf{t_C} \tag{1.1}$$

$$\mathbf{p} = \left[\frac{x_C}{z_C} f_x + C_x, \frac{y_C}{z_C} f_y + C_y \right] \tag{1.2}$$

where f_x and f_y are the respectively the orizontal and the vertical focal lenght and $[C_x, C_y]$ are the coordinates of the center of the image.

As discussed in [**?**], we can build several considerations on top of those two coupled equations :

- the relationship between image points and pose parameter is hightly non linear and the problem of retrieving the 3-D points from the 2-D image can have infinite solution in under-constrained situations [**?**];

- the correspondence between $\mathbf{q_B}$ and $\mathbf{p}$ is not knon a priori;

- the image coordinates need to be corrected for pixel's non-quadratism and lens distortion before using the foreametioned equations.

The pose estimation system thus needs the be capable of extracting the client features from the available image (image processing) to obtain measurements, namely $\mathbf{p}$. The extracted features then needs to be matched to the correspondent elements of a client model (model matching), namely $\mathbf{q_B}$. The unknown pose then has to be estimated based on the available measurements (pose estimation).
The architecture proposed in [**?**] solve the pose estimation problem by coupling the Weak Gradient Eliminator (WGE) technique with the Sobel edge detection to perform the image processing, uses feature synthesis to reduce the searh space for model matching and combines a P-n-P solver with the Netwon-Raphson (NR) method for pose estimation.

1.3   Host Company

This R&D project was developed at D-Orbit.
D-Orbit is a New Space company with solutions convering the entire life-cycle of a space mission, including mission analysus and design, engineering, manufacturing, integration, testing, launch, mission control and end of life decommisioning.
The company's competitive advantage is in the versatility of its launch and deployement services that can me tailored to the customer's needs, from the launch procurement of a single satellite using standard deployment strategies to the precise deployment of a full constrallation with ION satellite Carrier, a satellite dispenser developed and operated by D-Orbit.
ION Satellite Carrier can host any combination of CubeSat with a total volume of up to 48U and release them individually into distinct orbital slots, enabling delplyment schemes previously unavailable to satellite with no indipendent propulsion.
Committed to pursuin business modeal that are profitable, friendly for the environment, and socially beneficia, D-Orbit is the first certified B-Corp space company in the world.
Headquartered in Como, Italy, D-Orbit has subsidiaries in Lisbon, Portugal, Harwell, UK, and Washington DC, USA.

1.4   Structure of the Thesis

Chapter 2

State-of-the-art and Limitations

"We are just an advanced breed of monkeys on a minor planet of a very average star. But we can understand the Universe. That makes us something very special."

Stephen Hawking

2.1 Synthetic Image Generation for Spaceborne Applications

2.1.1 Professional Solutions

ESA PANGU

PANGU is a software developed in order to create synthetic planetary surface images, as much representative as possible, to aid the development of vision-based algorithms.[?]
PANGU is a nice software which is ready to use. It's use is permitted for free for users working on an ESA project, while non-ESA users have to contact STAR-Dundee to purchase PANGU with technical support.
PANGU can also be integrated with proprietary or OSS simulation tools and it gives the possibility to correctly simulate a space camera in all its aspects (so focal lengths, and other relevant parameters of the image). It renders the images using OpenGL and it can use GPU cores to accelerate the rendering.

Airbus Surrender

SurRender is a software developed by Airbus Defense and Space. The software handles various space objects such as planets, asteroids, satellites and spacecraft. It is capable of accommodating solar system-sized scenes without precision loss,

and optimizes the ray tracing process to explicitly target objects. It can operate in real time mode to be coupled with proprietary or OSS simulation tools and it gives the possibility to have an Hardware in The Loop simulation to test the responsiveness of the image processing subsystem. It gives the possibility to correctly simulate a space camera in all its aspects (so focal lengths, and other relevant parameters of the image). It parallelized and so can be ran on cloud platform to accelerate rendering times.

2.1.2   Low-Cost Solutions

SPEED dataset: image generation using OpenGL

URSO dataset: image generation using Unreal Engine 4

POV-Ray

POV-Ray it is an opensource ray-tracing tool. It does not offer a GUI for modeling objects, like Blender, but it can be used as Blender rendering engine to be able to have a 3D modeling environment to model our objects.
POV-Ray has also been used by a different number of people doing research work in the space field to generate images, for example it has been used under the ESA LunarSim study to render images of lunar surfaces. It can also be extended to correctly simulate images of spacecraft. It is a powerful software which let us define surfaces and materials relevant properties such as reflectivity, diffraction, specularity and brillance. Those parameters can be fine tuned to obtain an image as realistic as possible, under certain limits.
POV-Ray can be scripted in order to be used in conjunction with other softwares. Although does not let the user to add some sort of disturbance or noise to the generated images, those disturbances may be added by using some third party software such as MATLAB thanks to POV-Ray's ease of scriptability.
Up to a certain point, it also let us define some basic characteristic of the camera, such as the focal lengths, although it does not let us correctly simulate some other effects such as lens distorsions (which again, can be added using a third party software such as MATLAB).
POV-Ray major drawback are reported in [**?**], and are:

- Only a Lambertian reflectance model is possible;

- A uniform surface albedo is used and realistic albedo values cannot used;

- The extended illumination source (sun) can be modelled only as an array of point light sources or as an area light, which is a suboptimal solution;

- Background lighting (starlight) is cannnot modelled;

- Earthshine cannot be easily modelled;

- POV-Ray can produceshigh quality images but rendering is slow as many minutes (sometimes hours) are required to produce a single image;

Despite those limitations POV-Ray can been used to produce synthetic space imagery with an acceptable degree of accuracy for CV algorithm training.

2.2 Spaceborne Close-Proximity Relative Navigation

2.2.1 Pose estimation sensors

2.2.2 Pose estimation tecniques

Chapter 3

Synthetic image generation

"In math, you're either right or you're wrong."

Katherine Johnson

3.1 Mathematical Preliminaries

3.1.1 Reference Frames

In order to be able to correctly analyze to problem of image generation, five reference frames are of interest:

- Geocentric Inertial Frame (GCI)

- chaser body-fixed frame

- camera frame

- target model frame

- target body-fixed frame

The GCI frame has its origin at the center of mass of the Earth. This frame has a linear acceleration because of the Earth's circular orbit about the Sun, which however can be neglected for attitude analysis. It's axes are aligned with the mean North pole and the mean vernal equinox at some epoch.

The chaser and target body-fixed frames have their origins at the CG of both, respectively, and their axes are usually aligned with their respective principal axes. The origin of the camera frame instead coincides with the center of perspective projection.

The target model frame is fixed with respect to the body frame and often coincides

with it.

For what concerns this work, we will consider the camera frame to be coincident with the chaser body-fixed frame, and the target model frame to be coincident with the target body-fixed frame.

The transformation from one reference frame to another can be uniquely defined by means of a translation vector and a rotation matrix. The translation vector represents the relative positions between the two different frames origins and the rotation matrix is determined by a sequence of three rotations about three different linearly independent axis by three angles, according to the Euler's angle representation.

3.2   Image generation

The use of artificial images gives a complete control over the scene.

As stated in [**?**], the generated dataset should be as complete as possible in terms of metals and terrain features and illumination conditions.

A lack of realism in image generation can lead to incoherent results, not representative of real operative conditions and thus can lead to wrong results in terms of CV algorithm tuning.

A particular care is then required in the image generation process.

For the purpose of this work, a new procedure for the generation of realistic images, representative of a dataset taken by a monocular navigation camera during a close-proximity approach to targeg S/C has been developed.

Unsing the illustrated procedure, the user is able to create synthetic images of a target S/C given it's STL model, by fine tuning all the properties of the materials composing the target S/C.

Since there could be also cases in which the Earth can be behind the target S/C, the developed tool is also able to simulate Earth's presence at any given location. The tool is also able to the simulate the the athmosphere of the Earth and the cloud layer [**?**].

The developed tool couples a well known open source raytracer (POV-Ray) with MATLAB in order to archive a good degree of realism in the generated images.

3.2.1   Ray Tracing

What is ray tracing

Ray tracing is a rendering technique used for generating artificial images which relies on the concept of controlling the path of view lines which starts from the observer camera and ends to generic virtual objects and thus calculating the color of the object. What is really of crucial importance for our particular use case is that ray tracing is capable of re-creating some of nature's optical effects

through transparent and opaque surfaces as reflection and refraction, scattering, and dispersion phenomena (such as chromatic aberration). Due to this, ray tracing techniques can generate artificial images with a really high degree of photorealism. When the ray tracer renders the scene, a ray of light is traced for every pixel of the camera. Typically, each ray must be tested for intersection with some subset of the object in the scene. Once the ray has intercepted an object, the ray tracing algorithm will estimate the amount and the type of incoming light at the point of intersection, examine the material properties declared by the programmer and by combining those information will calculate the final color that should be attributed to the pixel. Several illumination algorithms and reflective or translucent materials may also require more rays to be re-cast into the scene in order to do the necessary computations. At first glance may seem cumbersome to start the ray from the observer towards the object rather than casting rays to the camera (as is in reality). However, doing so speeds up a lot the computation time, as most of the light rays present in a scene may never reach the eye of the observer, and so, all the time spent for tracing those would be useless. After either a maximum number of reflections or a ray traveling a certain distance without intersection, the ray ceases to travel and the pixel's value is updated.
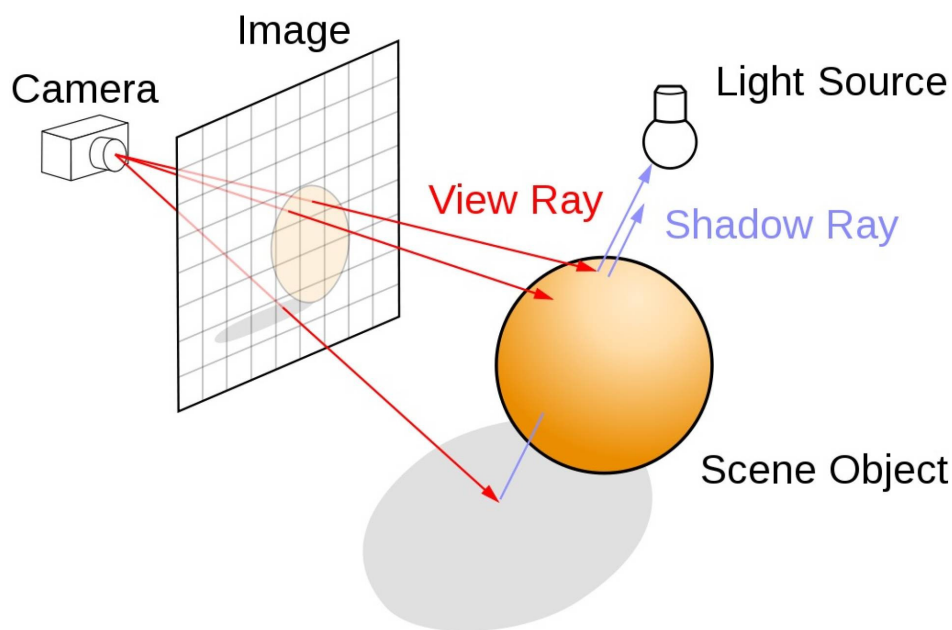

Figure 3.1: Raytracing: from the observer to the light source [**?**]

For more information regarding how ray tracing works, and ray tracing techniques see [**?**].

Ray tracing with POV-Ray

POV-Ray gives the programmer several options to customize both the look and feel and the optical properties of the represented objects and the medium that light passes trough.
POV-Ray offers the programmer the choice to use some predefined geometric shapes, like spheres or cubes; another option instead is to define surfaces of the objects trough meshes. This capability has been used widely by this project to model the spacecraft object.
Any surface can then be characterized by its own optical properties. Every object can have a color specified by an RGB triplet or can be wrapped with a texture.
The light source is not really an object. Light sources have no visible shape of their own. They are just points or areas which emit light and can be tuned to accomplish the wanted result, for example we can tune the intensity of the light and the light color by specifying the RGB triplet; any atmospheric effect like opaque gas presence (like smoke or clouds) and its rlative optical distortions can be modeled as well.

3.2.2   Environment Modeling

Earth Modeling

Earth modeling has been worked out in collaboration with Jacopo Guarneri. Here will follow a brief review of how Earth has been modeled taken from [**?**].
For modeling the Earth, the POV-Ray **sphere** object has been used, in conjunction with the **scale** feature, which allows to make the sphere become an ellipsoid.
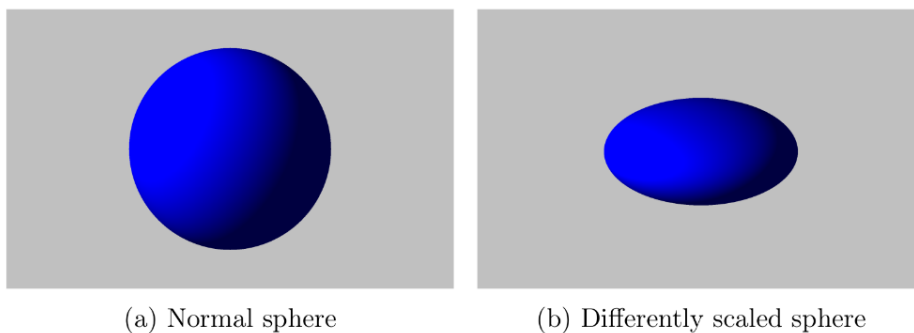

(a) Normal sphere   (b) Differently scaled sphere

Figure 3.2: Sphere manipulation with POV-Ray [**?**]

Once the 3-D object is created, the most natural choice one can think of is to wrap a 2-D texture of the Earth (**??**) on it, and this indeed is what has been done, using the high resolution (8K) texture of the Earth.
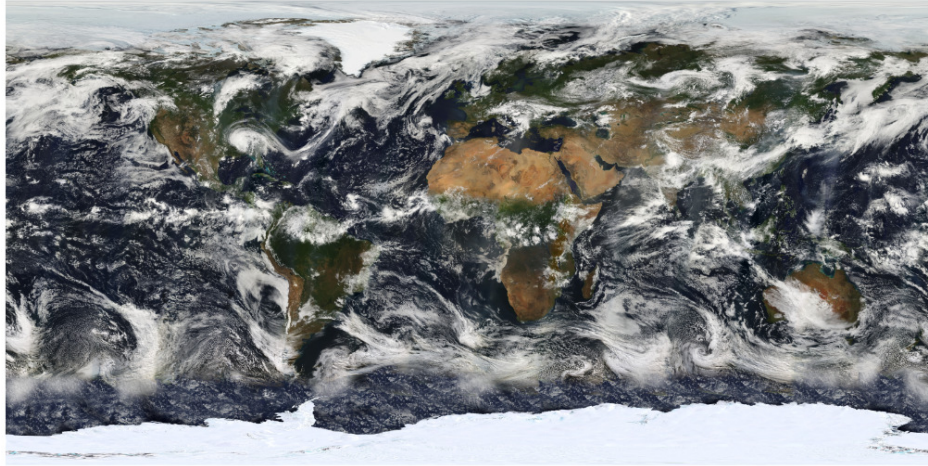
Figure 3.3: Initially chosen texture of the Earth

In **??** we can see a comparison of the synthetically generated image and an actual true image of the Earth as seen from the Apollo 11. From a first glance, used texture gives a good representation of what we should see when we look of a picture of the Earth taken from the space.

(a) POV-Ray representation of the Earth   (b) Apollo 11's picture of Earth

Figure 3.4: Comparison of synthetic Earth image with Apollo 11's picture

Despite the relatively good result, this way of modeling the Earth still haves some issues :

- since for all pictures we use the same texture, the clouds are sticked to their position on top of the surface of the Earth;

- there is no way to define different optical properties for the terrain and the seas;

- there is no way to try to simulate diffusion of sunlight in the atmosphere;

In the following, those issues will be addressed.

Cloud Layer

The fixed coupling of Earth surface and clouds is big problem for what concerns CV algorithms development, which should be trained to work in several different conditions, so, having the clouds always on the same region of the Earth despite the orientation is not acceptable.

The solution adopted in both this work and [**?**] relies on decoupling the Earth terrain layer and the cloud layer, specifying different optical properties for each layer, specify clouds relative rotation with respect to the terrain and coupling back everything together. Furthermore, oceans have been splitted too, in order to be able to set different optical properties for the seas.

For the terrain layer, a a true-color mercator image of the Earth has been used as a base, in this way every piece of the surface could possibly be visible in any picture.
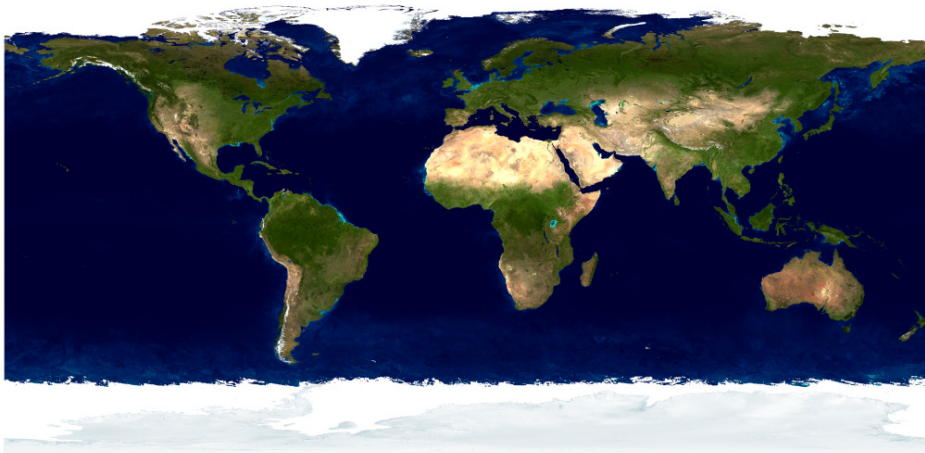

Figure 3.5: True Color Earth Mercator Image [**?**]

As said before, in order to be able to use different optical properties for water and terrains, a separate two-color mercator-projection image of the Earth where the water is black and the land is white has been used.
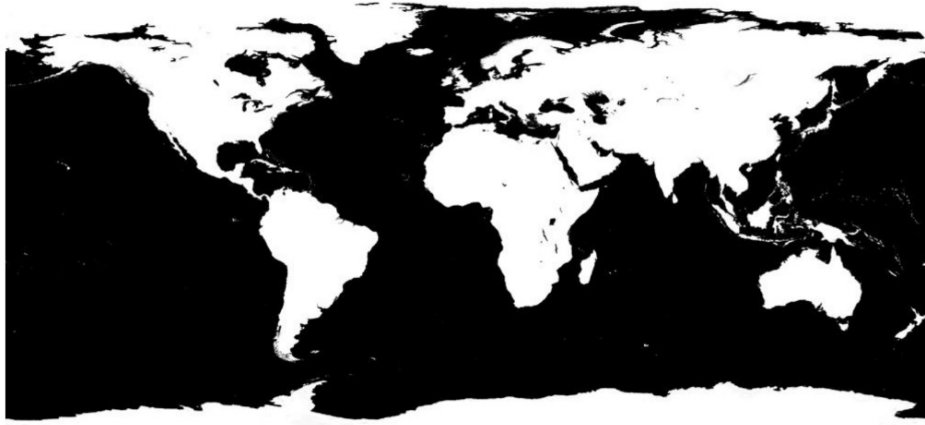
Figure 3.6: Landmask Mercator Image

In **??** the result of differentiating the optical properties for terrains and oceans is shown. Despite the fact that it may seems that there is only a small distinction between the two images (in particular, shinier oceans and darker forests), is still enough the make the Earth to seem more photorealistic, and it leave some space for further tuning.

(a) No differentiation of parameters   (b) Differentiation of parameters

Figure 3.7: Comparing images with no differential treatment between land and ocean and with differential treatment

The cloud layer is added on top of the cloudless surface and thanks to that, it can rotate with respect to the Earth by a prescribed angle set by the programmer. The cloud layer texture and the shape of the clouds itself always remains the same, but this can be partially mitigated by using different cloud textures.
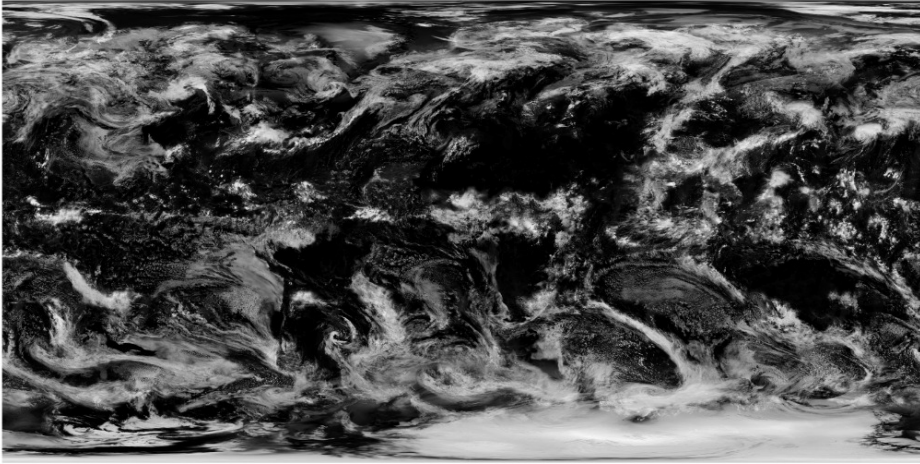
Figure 3.8: Two-color mercator image of Earth's cloud layer

The cloud texture used for this work (**??**) is not actually directly printed on the surface of the earth, but rather is extruded on a shell built around the sphere which defines the Earth, which has an inner radius equal to $R_{in} = 1.001 \cdot R_{Earth}$ and an outer radius equal to $R_{out} = 1.0002 \cdot R_{Earth}$. Those values have been found by taking as a reference the fact that low Earth clouds ranges from an altitude of $600\,\mathrm{m}$ to $15\,000\,\mathrm{m}$ [**?**]. Although higher or thicker clouds can be modeled, this will require longer rendering times. Of course, also for the cloud layer is possible to set custom optical properties, in order to make the clouds partially transparent, so that when there isn't a dense cloud area, the terrain behind is still visible under the white blanket.
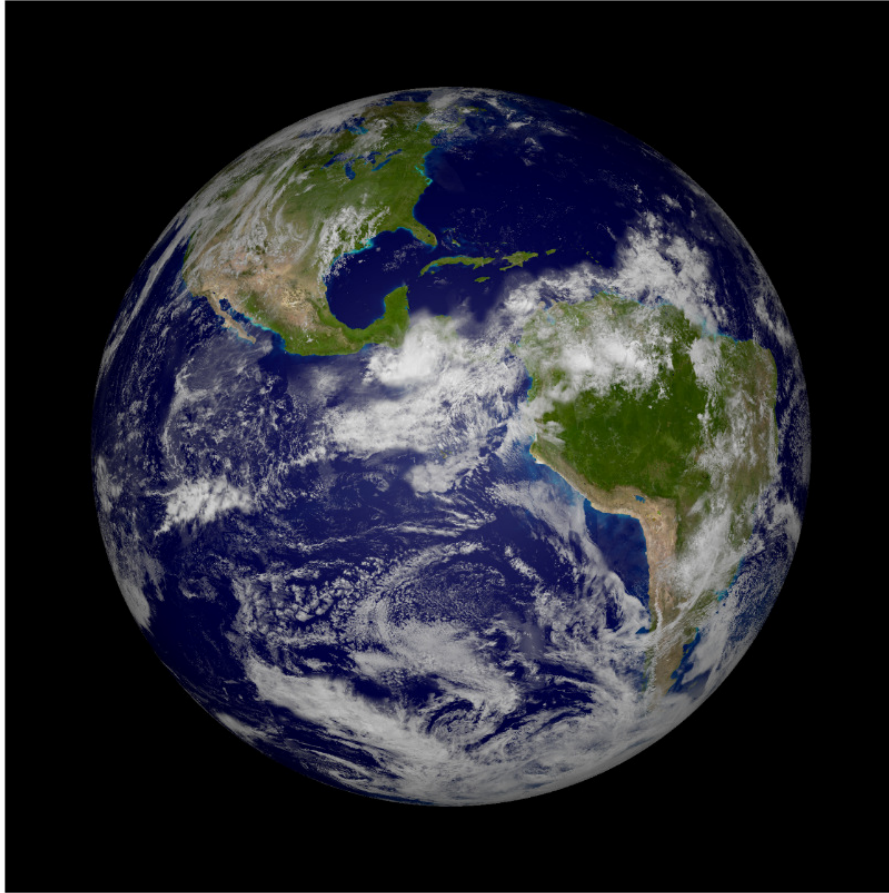
The result of adding the cloud layer can be seen in **??**

Figure 3.9: Earth's representation using cloud shell

Cloud Layer

Recreating the characteristic atmosphere presence around the Earth is of crucial importance for developing a CV algorithm for space applications, as it is needed in order to train the algorithm itself to work into a real-case scenario. The atmosphere's presence in fact would enlarge the aspect of the Earth in the image, and furthermore would stress the edge detection algorithms. To recreate the atmospheric shine effect, a strategy which is similar to the one adopted to model the cloud layer has been used. In fact, it has been modeled as a shell with a certain thickness of a transparent material with some scattering properties. For what concerns both this project and what has been done in [**?**], the gaseous layer was made only 25km thick. Despite the fact that the atmosphere should be visible up to many more kilometers, the computational load introduced by rendering a much high atmosphere is not negligible on a standard PC hardware, and so the image generation time would grow up exponentially, making the task of compiling a data-set of thousands of images very time consuming. In figure **??** can be seen the final result of adding the atmospheric model.
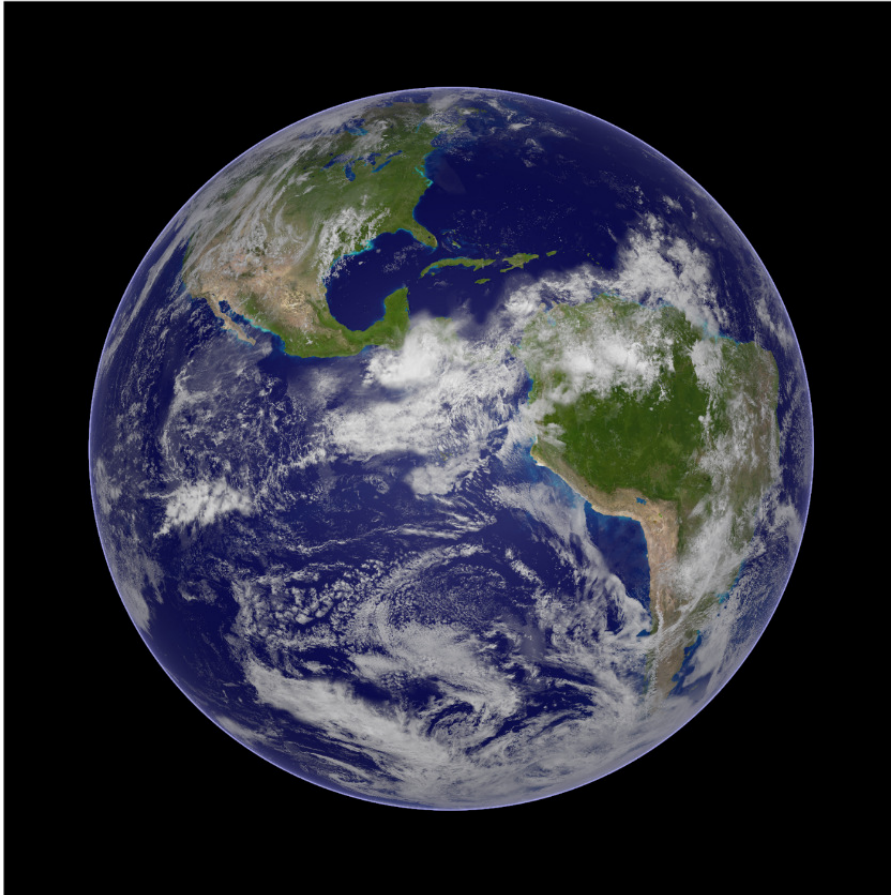
Figure 3.10: Earth with the atmosphere layer

In figure **??** instead is possible to view the artificially generated next to a real Earth picture taken by NASA's Suomi NPP on January 4, 2012. It can be seen that, despite the fact that the real image isn't perfectly reproduced (because some other factors should be known in order to be taken into account, such as exposure time), the synthetic image still provide an high degree of similarity with the real one.
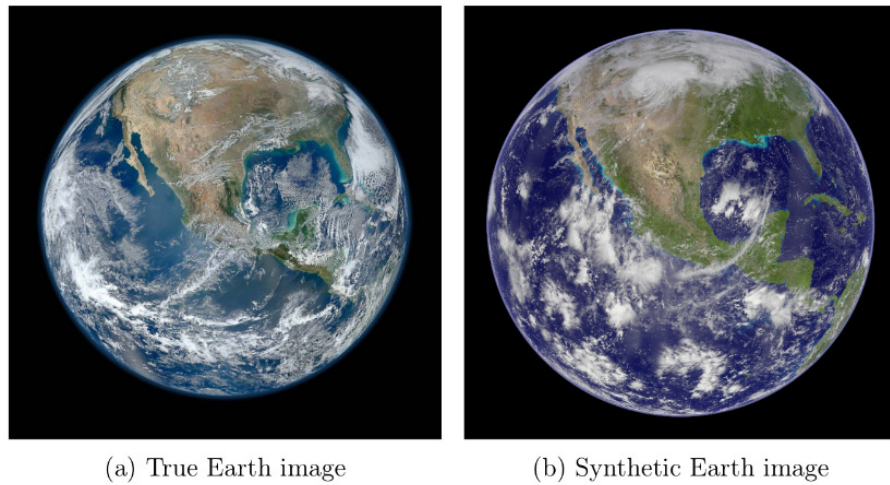
(a) True Earth image   (b) Synthetic Earth image

Figure 3.11: Comparison between true and final rendered Earth image

In table **??** are briefly resumed the values used to model the various layer of the Earth.

	Terrain	Oceans	Clouds	Atmosphere
Ambient	0.001	0.001	0.001	0.0001
Roughness	0.05	0.1	0.005	0.5
Brillance	1	1	1	1
Diffuse	0.85	0.85	1	0.6
Reflection	0	0.04, 0.25	0	0
Specular	0	0.1	0	0

Table 3.1: Optical parameters of Earth's different layers

Light Modeling

For an object to show up into the scene, it must be illuminated. There are two ways to illuminate an object with POV-Ray:

- use a standard light source

- use ambient light

The light source is controlled by the keyword **light_source**, which in turn accepts several modifiers. Light sources in POV-Rayhave no visible shape of their own. They are just points or areas which emit light.
The ambient light instead is controlled by the keyword **ambient** added to the **finish** modifier of an object, and it is used to simulate the light inside a shadowed area. We can think of ambient light like a kind of light that is scattered everywhere

in the room. It bounces all over the place and manages to light objects up a bit even where no light is directly shining. In our particular case, we can use the **ambient** option to simulate the illumation of the object due to spurious light sources (such as stars) or reflection from other bodies (like the Moon or other planets). In order to model the lightning condition of a true solar system, the light source has been modeled to resemble as much as possible the light emitted by the Sun. The solution adopted in this project and in [**?**] relies upon modeling the sun as an area light source through the option **area_light**. This allows to create a cluster of point-like light sources distributed on a disc (simulated by adding the circular option to the area light source) which has radius equal to the radius of the Sun, and placed at the exact distance which the Sun has from the Earth in the GCI frame. In order to cope with the fact that in reality the Sun is equal to a sphere of light and not a disc, the option orient has been used. When using orient, every object in the POV-Ray world would see the Sun's disc as oriented toward it, from any position around it. Furthermore, the option **jitter** has been used, which tells the ray-tracer to slightly move the position of each light in the area light to eliminate any shadow banding that may occur.

3.2.3   Tango Spacecraft Modeling

3D Model of the Spacecraft

The problem of modeling rather complex shapes with POV-Ray, such as can be a spacecraft, it was one of the most long and painful one during this work, which also required to patch POV-Ray source code, to prevent the ray-tracer to made assumption that aren't true. Obviously, the path of building the S/C using POV-Ray primitives was really not feasible, as many different S/C can have different shapes, and modeling them by using simpler shapes it is simply not possible. Furthermore, usually detaled 3-D CAD models of S/C are available which can be easily exported into STL format, so the focus has been putted into trying to understand how to translate those 3-D CAD models directly into POV-Ray code. Several open source and closed source software have been coupled together in order to produce trough POV-Ray a render of a given STL model. The procedure will be detailed in the following paragraphs. The Tango spacecraft has been modeled using the dimensions specified in [**?**], which will be here reported for ease of reading. The solar panel is represented by a polygon of 570mm x 759mm, while the spacecraft body instead is represented by a convex polyhedron of 560mm x 550mm x 300mm. The radio frequency antennas length instead is of 204mm. The origin of the CAD model is located in correspondence of the CG.
Using the aforementioned dimensions, the Tango spacecraft has firstly been reproduced using Autodesk Inventor. The result of the modeling procedure is shown in figure **??**.
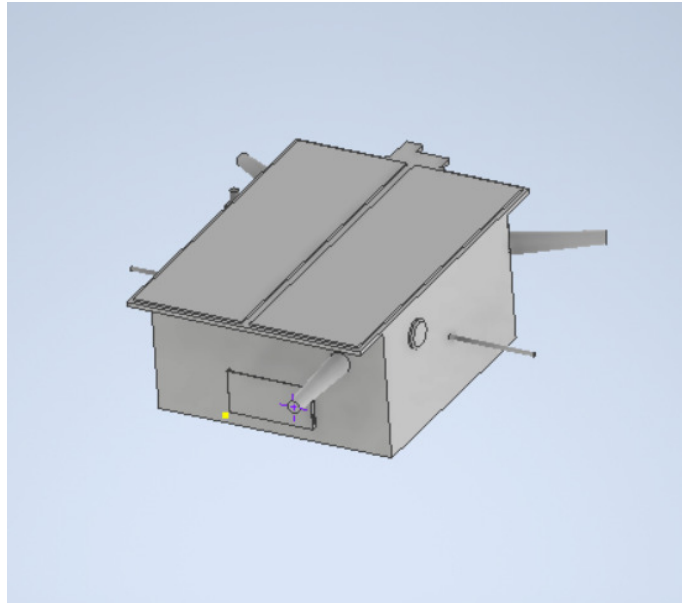
Figure 3.12: Tango S/C 3-D model

The 3-D CAD model can now be exported in STL format to be manipulated through other software.

Blender

Once the 3-D model of the Tango S/C was available, the most challenging task has been the one of rendering the S/C itself using POV-Ray at attitudes imposed by the user.
The first step for archiving that goal is to import the STL model of the S/C into Blender.
By exploiting the POV-Ray render add-on for Blender, it is possible to render any given STL file imported file using POV-Ray as rendering engine. The POV-Ray add-on will optionally save the generated SDL code used to render the scene.
The generated code however, will threat the entire 3-D model as a whole, generating one giant POV-Ray mesh2 object, which is something which cannot be easily managed. Just as an example, would be impossible to assign to the different parts of the S/C different optical parameters or textures.
So, to workaround this limitation, it is a good practice to first split the different surfaces of the 3-D model in different different children objects (or children surfaces), and only after render the scene in order to get the POV code. In that way, the POV-Ray render add-on for Blender will generate a mesh2 object for each children object created in Blender. This will enable us to set different material properties for each children surface or to apply different textures to different surfaces. For the purpose of this work, the original STL model has been subdivided into thirty children object, each one with its own optical parameters, as can be seen from
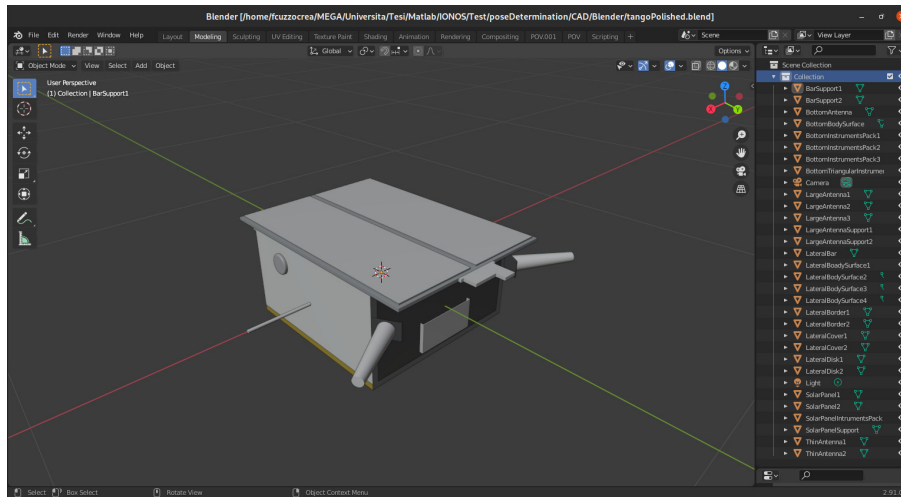
figure **??** .

Figure 3.13: Tango S/C 3-D model in Blender

The Blender POV-Ray add-on also let the user to inject custom POV code
(figure **??**) into the auto-generated one, which can be useful especially for adding
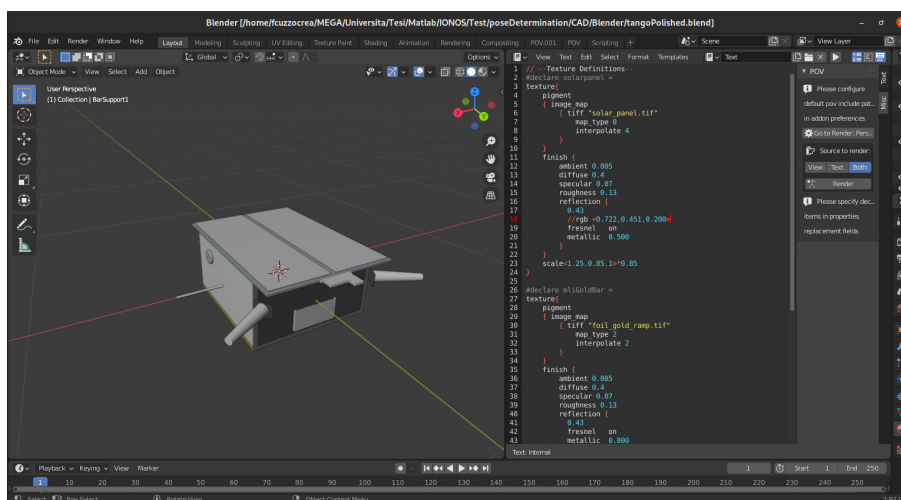textures, for example to the solar panels, as it has been done into this project.

Figure 3.14: Add custom POV code into Blender

The end results is showed in figure **??**
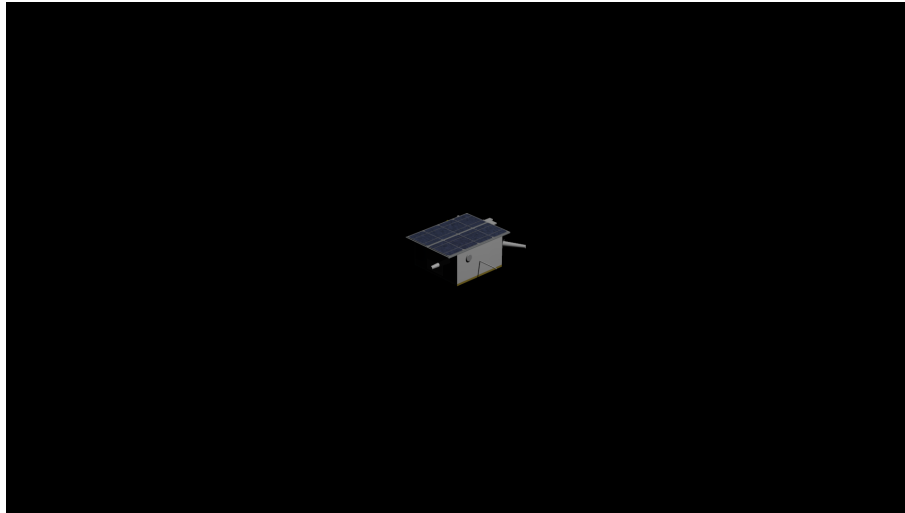
Figure 3.15: Tango S/C rendered using POV-Ray Blender add-on

POV-Ray

The major issue of the code generated from the POV-Ray Blender add-on is that is composed of several separated mesh2 objects which makes almost impossible to rotate the whole object by imposing a given attitude matrix, since one is supposed to rotate all the mesh2 objects by hand.

In order to workaround this limitation, from all the mesh2 objects which have been generated from POV-Ray Blender add-on are merged into one single **merge** object. The **merge** POV-Ray operation allows to bind two or more shapes into a single entity that can be manipulated as a single object, which is exactly what we want. The new object created by the merge operation can be scaled, translated and rotated as a single shape. The entire merge can share a single texture and optical parameters but each object contained in the union may also have its own texture and optical parameters, which will override any texture statements in the parent object. So, all the mesh2 objects which describes the S/C surfaces are merged into a single big (21K LoC) **spacecraft merge** object.

To ease the usage of the **merge** object, a POV-Ray include file it is created, with the sole purpose of containing the **spacecraft merge** object. The include file is read in as if it were inserted at that point in the file. Using include is almost the same as cutting and pasting the entire contents of this file into the scene. This allow to define the **spacecraft merge** once and call it from any other POV file just like any other predefined object is called, and so, it is possible to manipulate its position and orientation in a much more easier way.

In table **??** are briefly resumed the optical parameters used to model the different part of the S/C.

	Solar Panels	Antennas	Main Body
Ambient	0.0	0.25	0.25
Roughness	0.13	0.0005	0.0005
Brillance	-	3.15	3.15
Diffuse	0.3	0.95	0.99
Reflection	0.23, 0.5	0.65, 1	0.65, 1
Specular	0.04	0.96	0.96
Phong	-	0.43	0.43
Phong Size	-	25	25

Table 3.2: Optical parameters of S/C different parts

3.2.4   Camera Modeling

In POV-Ray's camera environment, the programmer can set all relevant camera parameters, which will be then used to simulate the camera trough which the scene will be rendered.

The most meaningful parameters which can be modeled are the **location**, the **direction** of the boresight axis (where is the camera looking at with **look_at**), the view angle and the direction of the camera reference frame (by using **up** and **right** keywords).

The major issue which has been faced when modeling the camera in POV-Ray is the fact that the program defaults to a left handed coordinate system to describe the scene, while all other software (like Autodesk Inventor, Blender) are using a right handed coordinate system.

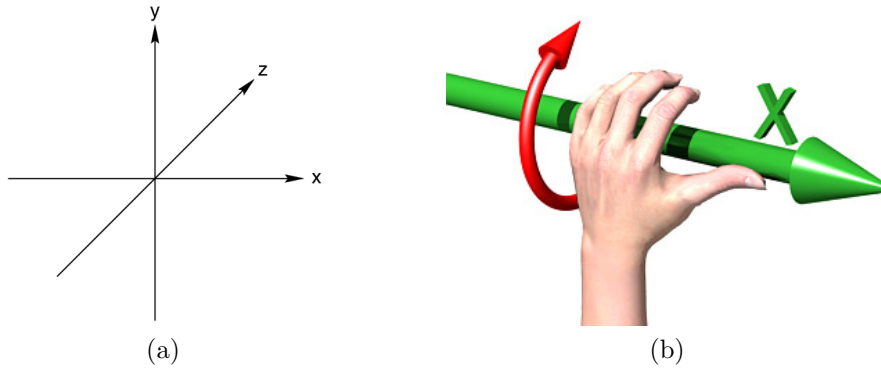(a)   (b)

Figure 3.16: POV-Ray coordinate system

Moreover, the right handed coordinate system is used also to model the orbit that the spacecraft will follow and the spacecraft attitude from Euler equations. It is possible to trick POV-Ray to behave like it using a right handed coordinate system by acting on the **right** vector of the camera environment. The camera

right vector describes the direction to the right of the camera, so, in practicte, tells POV-Ray where the right side of the screen is. Therefore, the sign of the x component of the **right** vector can be used to determine the handedness of the coordinate system in use.

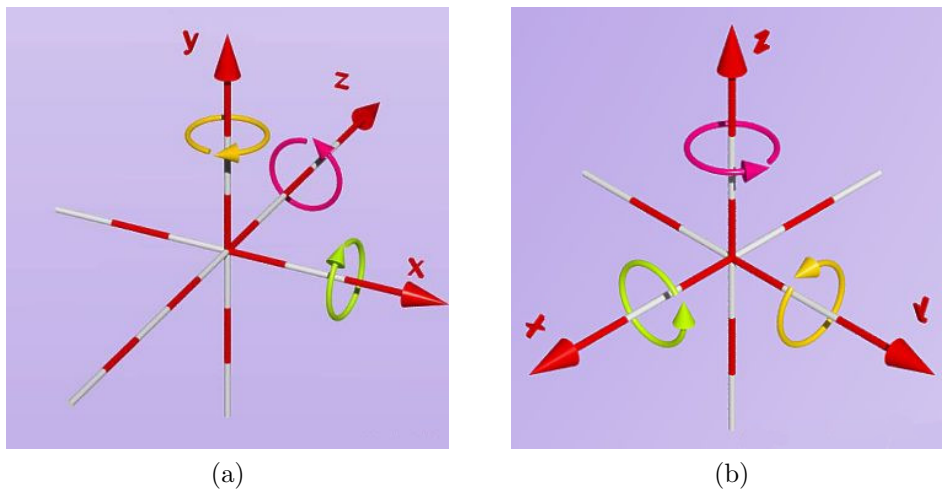(a)   (b)

Figure 3.17: Right Handed Coordinate System and Left Handed Coordinate System

By default POV-Ray use a positive x value in the **right** vector. This means that the right side of the screen is aligned with the +x-direction. By using a negative x value in the **right** vector instead the right side of the screen will be aligned to the -x-direction, and the coordinate system will be right handed.
Doing only that however left us having the y axis as the one pointing upward and the z axis as the one point in the direction which goes outside the screen.
To have a more comfortable, which also uses the same axes of the GCI reference frame, we can flip y and z axis by overriding the **sky** vector. By default, in fact, POV-Ray uses <0,1,0> as **sky** vector. By redefining it as <0,0,1> POV-Ray will roll the camera until the top of the camera is in line with the sky vector, giving us the desired result.
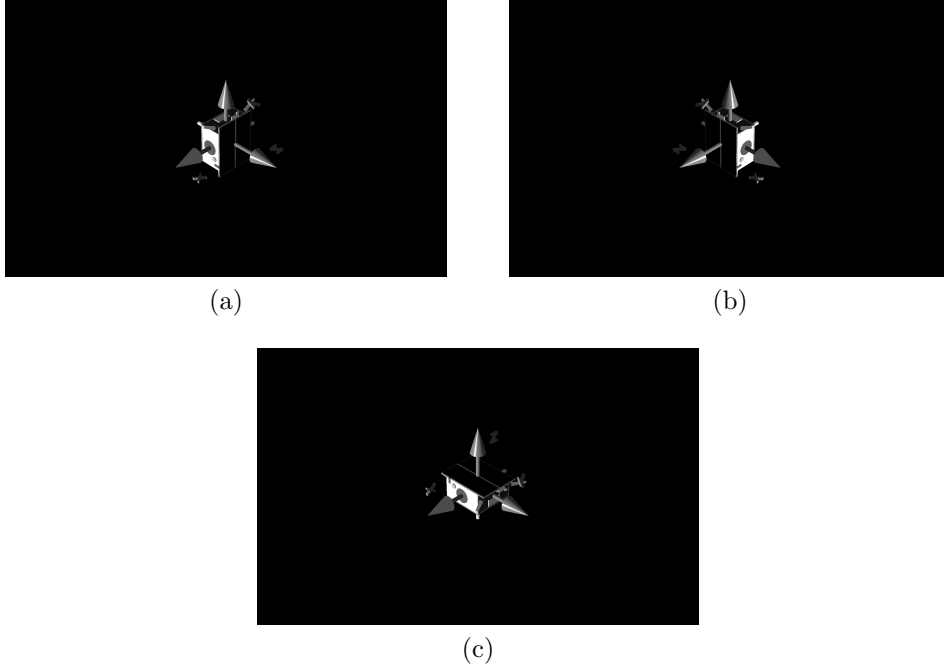
(a)

(b)

(c)

Figure 3.18: Right Handed Coordinate System and Left Handed Coordinate System

In order to rightly simulate a real camera, the POV-Ray camera aperture angle has been computed by assuming the intrinsic properties of a real camera, a Point Grey Grasshopper 3, equipped with a Xenoplan 1.9/17 mm lens, which is the same camera employed to capture the SPEED dataset [?].

Parameter	Description	Value
N_u	Number of horizontal pixels	1920
N_v	Number of vertical pixels	1200
f_x	Horizontal focal length	17.6 mm
f_y	Vertical focal length	17.6 mm
d_u	Horizontal pixel length	5.86×10^{-3} mm
d_v	Vertical pixel length	5.86×10^{-3} mm

Table 3.3: Parameters of the camera used to capture the SPEED images [?]

By assuming a CCD sensor which only has square pixels we can obtain:

$$A.R. = \frac{N_u}{N_v} \tag{3.1}$$

$$CCD_{size} = d_u \cdot N_u \tag{3.2}$$

$$\alpha = 2 \cdot \arctan \frac{CCD_{size}}{2 \cdot f_x} \tag{3.3}$$

where $A.R.$ is the Aspect Ratio of the picture, which is passed as first component **right** vector (with the negative sign, as described before), and α is the aperture angle which will be input in POV-Ray. Using the parameters detailed in table **??** we can compute:
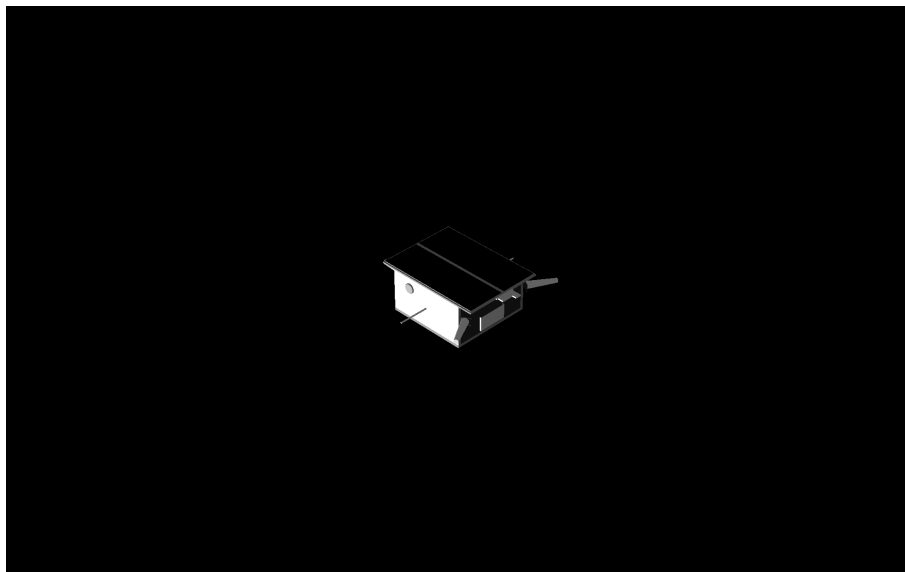
- $A.R. = 1.6$

- $\alpha = 35.4515°$

Figure 3.19: Tango S/C rendered using table **??** parameters

Adding the noise

Finally, for augmenting the "realness" of an image generated though POV-Ray, the image needs to be post-processed using MATLAB. The image so is input in MATLAB and two different noises are applied through the imnoise command : speckle noise ($\sigma^2 = 0.004$) and Gaussian white noise ($\sigma^2 = 0.003$).
The final result can be seen in image **??**.

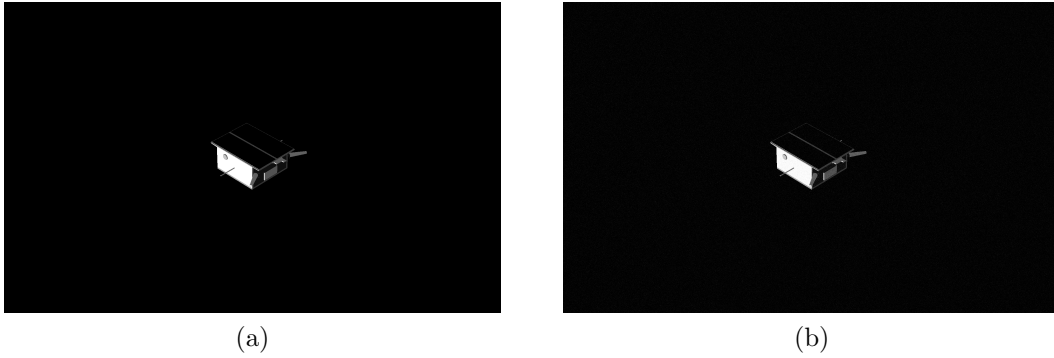<div align="center">(a)   (b)</div>

Figure 3.20: Comparison between image without noise and image with speckle and Gaussian white noise

3.3 MATLAB integration

3.3.1 Random Attitude Image Generation

3.3.2 Pseudo-random Attitude Image generation

3.3.3 Caveats

Chapter 4

The SVD architecture for pose initialization

"Prediction is very difficult, especially if it's about the future."

Niels Bohr

4.1   Mathematical Preliminaries

4.1.1   Pinhole Camera Model

4.1.2   Image derivatives

4.1.3   The Hough Transform

4.1.4   Perspective-n-Point problem

4.2   Feature-based pose estimation implementation

4.2.1   Architecture

4.2.2   Image processing subsystem

Feature Detection

Feature Synthesis

Perceptual Grouping

4.2.3   Model Matching and Pose Determination

Feature Correspondence (?)

Pose Determination

Chapter 5

Results

"Most good programmers do programming not because they expect to get paid or get adulation by the public, but because it is fun to program."

Linus Torvalds

5.1   Syntetic Dataset Validation

5.2   SVD Architecture Validation

Conclusions

Appendix A

First appendix: Attitude and Orbit Simulator

In this appendix the kinematic and dynamic representation used for the simulation of the attitude of the target spacefrat will briefly be described.

A.1 Keplerian Motion

The dynamics of the CG of a rigid body is given by Newton equation of motion stating that the variation in time of the linear mentum is equal to the external forces applied to the body, with respect to an inertial reference frame. Thus :

$$\frac{d}{dt}(m\mathbf{v}) = \sum_{i=1}^{n} \mathbf{f_i} \tag{A.1}$$

where m is the mass of the body, $\mathbf{v}$ its velocity and $\mathbf{f_i}$ the forces applied to the system. Then, for a rigid body orbiting around a single massive body, the main force to take into account is the gravitational pull that can be modelled accordingly to Newton law of gravitation as follows :

$$m\ddot{\mathbf{r}} = -\frac{\mu m}{\|\mathbf{r}\|^3}\mathbf{r} + \mathbf{f} \tag{A.2}$$

where μ is the gravitational constant of the main attractor, $\mathbf{r}$ the position vector of the orbiting body computed from the main attractor CG and $\mathbf{f}$ the sum of other forces applied to the system. The underlying assumption is to consider the main attractor to be still or moving in linear constant motion, which is never the case. Such assumptions holds well enough for many problem of interest. Considering null or negligible other forces it follows that the system motion is central, thus the angular momentum is conserved.

Such quantity, for this system, is defined as follows

$$\mathbf{h} = \mathbf{r} \wedge \mathbf{r} \tag{A.3}$$

where $\mathbf{v}$ is the velocity, derivative of the position vector $\mathbf{r}$ expressed in the said reference frame.

Crossing **??** with the angular momentum and considering that the gravitational field is conservative, it is possible to determine the position of the orbiting body in time through six parameters that represent the analytical solution of the restricted two body problem. For this research the influence of other massive bodies is not taken into account as for many of the applications here considered can be analysed considering satellites to be small bodies close to the planet.

The most used set of parameters are often referred to as Keplerian parameters, however different parametrization are possible. Of these six constant two represent the shape of the orbit, which must be a conic according to Kepler's studies and Newton's formulation, three identify the orientation of the orbit in a 3-D space and the last one links the position along the orbital with time. The shape is identified by the semi-major axis a of the conic and the eccentricity e, restricted to be between zero and one for closed orbits, being zero for circular orbits. In the reference frame with z axis aligned with angular momentum and x axis aligned with the minimum orbital distance (eccentricity vector) the position vector can be written as follows

$$\mathbf{r_{orb}} = \frac{\frac{\|h\|^2}{\mu}}{1 + ecos\theta} \begin{Bmatrix} cos\theta \\ sin\theta \\ 0 \end{Bmatrix} = \frac{a(1-e^2)}{1 + ecos\theta} \begin{Bmatrix} cos\theta \\ sin\theta \\ 0 \end{Bmatrix} \tag{A.4}$$

Then the position vector $\mathbf{r_{orb}}$ in this frame can be translated back into the inertial $\mathbf{r}$ by using three sequential rotations in the order z - x - z according to the values of the other three parameters: argument of pericenter ω , inclination i and right ascension of the ascending node Ω.

A.2   Dynamics

A.2.1   Euler Equations

The dynamics of a rigid body which is tumbling into space can be modeled by mean of the well known Euler equations, having in mind that such equation is expressed in a non-inertial reference frame attached to the body frame :

$$\omega_{\mathbf{B}} = (\mathbf{I_B})^{-1}[\mathbf{L_B} - \omega_{\mathbf{b}} \wedge (\mathbf{I_B}\omega_{\mathbf{b}}) \tag{A.5}$$

where ω_B is the angular velocity vector of the spacecraft in body frame, I_B is the inertia tensor of the spacecraft in body frame and L_B are the external torques acting on the spacecraft due to external disturbances and control torques.

A.3   Direct Cosine Matrix

The direct cosine matrix, or attitude matrix, gives the transformation of a vector from a reference frame N to another reference frame O :

$$\mathbf{r_O} = \mathbf{A_{ON} r_N} \tag{A.6}$$

So, if we consider the spacecraft body frame and the inertial frame, then we can write the relation between the two frames as :

$$\mathbf{r_B} = \mathbf{A_{B/N} r_N} \tag{A.7}$$

As it is demonstrated in Ref. [**?**], we can express the time dependence of the attitude matrix by writing the rotation from the body frame to the inertial frame as :

$$\dot{A}_{B/N} = -[\omega_{B/N} \times] A_{B/N} \tag{A.8}$$

where $[\omega_{B/N} \times]$ is the skew-symmetric cross product matrix containing the components of the angular velocity vector :

$$[\omega \times] = \begin{bmatrix} 0 & -\omega_{B/N_3} & \omega_{B/N_2} \\ \omega_{B/N_3} & 0 & -\omega_{B/N_1} \\ -\omega_{B/N_2} & \omega_{B/N_1} & 0 \end{bmatrix}$$

Thus, by integrating this relation, we can get full attitude at every iteration.

A.3.1   Environmental Disturbances

The external disturbances acting on spacecraft placed in a LEO orbit are basically four and are due to :

- Gravity Gradient

- Magnetic Field

- Solar Radiation Pressure

- Aerodynamic Drag

Details about how those torques have been mathematically modeled will be given in the following sections.

Gravity Gradient

Any non-symmetrical rigid body in a gravity field is subject to a gravity-gradient torque. If we consider a rigid spacecraft, the torque due to the gravity gradient about the spacecraft's center of mass can be modeled as :

$$\mathbf{L_{gg}} = \frac{3\ mu}{r^3}\mathbf{n} \wedge (\mathbf{I}\ \mathbf{n}) \tag{A.9}$$

where μ is the Eart's gravitational constant, $\mathbf{r}$ is the radius vector from the center of the Earth, thus $r \equiv \|\mathbf{r}\|$, $\mathbf{I}$ is the inertia tensor in body frame and $\mathbf{n}$ is the body frame representation of a nadir-pointing unit vector.
Further details about the model can be found in reference [**?**].

Earth's Magnetic Field

The torque generated by a magnetic dipole $\mathbf{m}$ in a magnetic field $\mathbf{B}$ is

$$\mathbf{L_{mag}} = \mathbf{m} \wedge \mathbf{B} \tag{A.10}$$

where $\mathbf{B}$ is the magnetic field in the body frame. The most basic source of a magnetic dipole is a current loop. A current of I amperes flowing in a planar loop of area A produces a dipole moment of magnitude m=IA in the direction normal to the plane of the loop and satisfying a right-hand rule. When $\mathbf{m}$ is in Am^2 and the magnetic field is specified in Tesla, Eq. **??** gives the torque in Nm. If there are N turns of wire in the loop, the dipole moment has magnitude m=NIA (such as the case of a magnetic torquer). To model $\mathbf{B}$ either the full IGRF model or the simple dipole model can be used.
For what concerns this work, the full IGRF model truncated to the 10th order has been used. Further details about the model can be found in reference [**?**]

Solar Radiation Pressure

Solar radiation pressure acting on the surfaces of the spacecraft causes a disturbance torque that in general, cannot be neglected for orbits higher than 800 km, so it has been taken into account in this work. The SRP torque is zero zero when the spacecraft is in the shadow of the Earth or any other body, of course. To take into account the effect of solar radiation pressure on the spacecraft, the spacecraft's surface can be modeled as a collection of N flat plates of area S_i, outward normal $\mathbf{n_b}$ in the body coordinate frame, specular reflection coefficient ρ_s, diffuse reflection coefficient ρ_d and absorption coefficient ρ_a; those coefficients must sum to unity. For what concerns this work, only ρ_s and ρ_d have been considered, since all the absorbed radiation is emitted as thermal radiation, although not necessarily at the same time or from the same surface as its absorption. For an accurate modeling of thermal radiation we must also known the absolute temerature and the emissivity

of each surface. We can define the spacecraft-to-Sun unit vector in the spacecraft's body frame as :

$$\mathbf{s_b} = \mathbf{A_{B/N}s_i} \tag{A.11}$$

where $\mathbf{A_{B/N}}$ is the attitude matrix and $\mathbf{s_i}$ is the spacecraft-to-Sun unit vector in the GCI frame. We can define the angle between the Sun vector and the normal exiting from the normal to the i-th plate as :

$$cos(\theta_{SRP}^i) = \mathbf{n}_B^i \cdot \mathbf{s_b} \tag{A.12}$$

The SRP force on the i-th plate can be expressed as :

$$\mathbf{F}_{SRP} = -P_{Sun}A_i \left[2 \left(\frac{\rho_d^i}{3} + \rho_s^i cos(\theta_{SRP}^i) \right) \mathbf{n}_B^i + (1 - \rho_s)\mathbf{s_b} \right] max(cos(\theta_{SRP}^i), 0) \tag{A.13}$$

where P_{Sun} is the solar radiation pressure. The Solar radiation pressure torque acting on the spacecraft is then given by :

$$\mathbf{L}_{SRP}^i = \sum_{i=1}^{n} \mathbf{r}_i \times \mathbf{F}_{SRP}^i \tag{A.14}$$

where $\mathbf{r}_i$ is the vector from the spacecraft center of mass to the centre of pressure of the SRP on the i-th face. In this formulation we are not considering the albedo radiation coming from the Earth and from the Moon. Further details on how the solar radiation pressure, the spacecraft-to-Sun unit vector and the eclipse condition have been modeled can be found in reference [**?**].

Aerodynamic Drag

Aerodynamic torque is generally computed by modeling the spacecraft as a collection of N flat plates of area A_i and outward normal unit vector $\mathbf{n_B}$ expressed in the spacecraft body-fixed coordinate system. The torque depends on the velocity of the spacecraft relative to the atmosphere, which is not simply the velocity of the spacecraft in the GCI frame, because the atmosphere is not stationary in that frame. The most common assumption is that the atmosphere co-rotates with the Earth. The relative velocity in the GCI frame is then given by :

$$\mathbf{v_{relI}} = \mathbf{v_I} + [\omega_{\oplus}\times]\mathbf{r_I} \tag{A.15}$$

where $\mathbf{r_I}$ and $\mathbf{v_I}$ are the position and velocity of the spacecraft expressed in the GCI frame. The Earth's angular velocity vector is $\omega_{\oplus} = \omega_{\oplus}[001]'$ with $\omega_{\oplus} =$

0.000 072 921 158 553 rad/s. The velocity in the body frame is the computed as :

$$\mathbf{v_{relB}} = \mathbf{A_{B/N}} \begin{bmatrix} \dot{x} + \omega_{\oplus}y \\ \dot{y} - \omega_{\oplus}x \\ \dot{x} \end{bmatrix} \tag{A.16}$$

The inclination of the i-th plate WRT the relative velocity is given by :

$$cos(\theta^i_{aero}) = \frac{\mathbf{n}^i_B \cdot \mathbf{v}_{rel\ B}}{\|\mathbf{v}_{rel}\|} \tag{A.17}$$

The aerodynamic force on i-th plate in the flat plate model is

$$\mathbf{F}^i_{aero} = -\frac{1}{2}\rho C_D \|\mathbf{v}_{rel}\| \mathbf{v}_{relB}\ S_i\ max(cos(\theta^i_{aero}), 0) \tag{A.18}$$

where ρ is the atmospheric density, and C_D is the drag coefficient. ρ can be modeled by mean of the well known exponential decaying model for the atmospheric density :

$$\rho = \rho_0 e^{(-(h-h_0)/H)} \tag{A.19}$$

where ρ_0 and h_0 are reference density and height, respectively, h is the height above the ellipsoid and H is the scale height, which is the fractional change in density with eight. The value of ρ_0, h_0 and H changes with h. The values used to perform the simulation are the one given in [?]. The actual torque due to the aerodynamic drag can be computed as :

$$\mathbf{L}^i_{aero} = \sum_{i=1}^{n} \mathbf{r}_i \times \mathbf{F}^i_{aero} \tag{A.20}$$

where n is the number of faces and $\mathbf{r}_i$ is the vector from the spacecraft center of mass to the center of pressure on the i th face.

Appendix B

Second appendix: Random Rotation Matrix Generation